# EMPIRICAL MODELLING AND GREY RELATIONAL OPTIMIZATION OF WIRE ELECTRIC DISCHARGE MACHINING OF Ni51.59Ti SHAPE MEMORY ALLOY

UDC:621.9.048:669.24/29
Original scientific paper https://doi.org/10.46793/adeletters.2025.4.3.3

**Thakur Singh[1], Pradeep Kumar Karsh[2*], Prabhakar Zainith[1]**

[1]Department of Mechanical Engineering, Shivalik College of Engineering, Dehradun, India
[2]Department of Mechanical Engineering, Parul Institute of Engineering & Technology, Parul University, Vadodara, India

**Abstract:**
In this study, Ni51.59Ti shape memory alloy (SMA) was machined using Wire Electric Discharge Machining (WEDM) to investigate and optimize the influence of key process parameters like spark on-time ($S_{ON}$), spark off-time ($S_{OFF}$), servo voltage ($S_V$), and wire feed ($W_F$) on material removal rate (MRR) and surface roughness (SR). A total of 29 experiments were conducted using the Box-Behnken design (BBD) under the Response Surface Methodology (RSM) framework. Quadratic regression models were developed for MRR and SR, and Analysis of Variance (ANOVA) revealed that $S_{ON}$ had the most significant effect on both responses, followed by $S_{OFF}$, $S_V$, and $W_F$. The predictive models demonstrated high accuracy with $R^2$ values of 0.9609 for MRR and 0.9668 for SR, confirming their reliability for parametric predictions. To address the multi-objective nature of the problem, Grey Relational Analysis (GRA) was also employed to determine the optimal parameter settings, achieving $S_{ON}$ = 115 µs, $S_{OFF}$ = 60 µs, $W_F$ = 9 mm/min, and $S_V$ = 70 V. Under these optimized conditions, a favourable trade-off between maximum MRR and minimum SR was achieved, as verified by confirmation experiments with minimal error. The study highlights that increasing spark on-time and reducing spark off-time significantly enhance MRR while maintaining acceptable surface quality. This work demonstrates the effectiveness of integrating RSM with GRA for WTEM parameter optimization, offering a robust framework for machining complex and hard-to-cut shape memory alloys. The findings provide a valuable reference for extending hybrid optimization techniques such as machine learning, genetic algorithms, or ANFIS to further improve process efficiency and surface integrity in advanced manufacturing of NiTi-based components.

**ARTICLE HISTORY**
Received: 28 June 2025
Revised: 22 August 2025
Accepted: 4 September 2025
Published: 30 September 2025

**KEYWORDS**
Wire EDM, Shape memory, Optimization, Titanium alloys, GRA, RSM

## 1. INTRODUCTION

Wire Electrical Discharge Machining (WEDM) is a widely recognized non-traditional machining technique that utilizes a continuously fed metallic wire as an electrode to cut electrically conductive materials with extreme precision [1]. The process is based on controlled electrical discharges between the wire and the workpiece, which erode material without any direct contact, as shown in Fig. 1. A dielectric fluid, typically deionized water, surrounds the cutting zone to cool the wire, remove debris, and maintain the required gap for spark generation. This non-contact nature eliminates mechanical forces, reducing the risk of tool wear, distortion, and residual stresses during machining. WEDM is particularly suited for machining complex profiles, sharp edges, and high-hardness materials, such as

*CONTACT: Pradeep Kumar Karsh, e-mail: pradeepkarsh@gmail.com

tool steels, titanium alloys, super alloys, and composites. Its ability to achieve high-dimensional accuracy and superior surface finish has made it an essential process in aerospace, medical device manufacturing, mold and die making, and precision engineering applications. Furthermore, the use of thin wires (0.05–0.3 mm) enables the machining of fine details and minimal corner radii, making WEDM superior to many conventional techniques for intricate geometries [2,3]. However, the process is inherently energy-intensive due to low material removal rates (MRR), often requiring significantly more energy compared to traditional machining processes. The performance of WEDM is influenced by various input parameters, such as pulse on-time, pulse off-time, wire tension, wire feed rate, and discharge energy. Improper selection of these parameters can lead to sub-optimal outcomes, including poor surface finish, excessive wire wear, or inefficient energy consumption [4,5]. Despite significant advancements, research on optimizing WEDM parameters for improved energy efficiency and surface quality remains limited. While most studies have focused on maximizing MRR and minimizing surface roughness, few have explored the trade-offs between energy consumption and machining performance. Addressing these gaps is critical to developing sustainable WEDM processes that balance productivity, quality, and energy efficiency.

Many researchers have investigated the optimization of WEDM process parameters using various statistical and intelligent techniques. Scott et al. [6] formulated a multi-objective optimization model for WEDM, focusing on maximizing metal removal rate (MRR) and improving surface finish quality. Using factorial design and non-dominated point analysis through explicit enumeration and dynamic programming, the best control settings were effectively identified. González-Rojas et al. [7] applied Taguchi's L27 orthogonal array to optimize WEDM of AISI D2 steel, achieving an 8% reduction in energy consumption and a 1% improvement in surface roughness compared to baseline values, demonstrating the efficiency of the approach. Srivastava et al. [8] optimized WEDM parameters for EN-24 steel, revealing that peak current has a dominant influence on both MRR and surface roughness. The optimum settings for maximum MRR (7.701 $mm^3$/min) were *Ip* = 5 A, *Ton* = 20 µs, and *Toff* = 15 µs, whereas the best surface integrity (*Ra* = 6.39 µm) was obtained at *Ip* = 1 A, *Ton* = 10 µs, and *Toff* = 5 µs. El-Bahloul [9] showed that both RSM and ANN effectively predict MRR and SR for AISI 304 steel in WEDM, with ANN demonstrating higher accuracy. Using fuzzy logic, the optimal parameters were *Ton* = 25 µs, *Toff* = 5 µs, and *Ip* = 6 A, achieving maximum MRR and minimum surface roughness. Seshaiah et al. [10] optimized WEDM parameters for machining complex stainless steel 304 geometries using RSM. The study observed that selecting optimal wire speed, wire tension, discharge current, dielectric flow, and pulse timing significantly enhanced MRR and surface finish. Natarajan et al. [11] highlighted the influence of pulse interval, pulse duration, wire feed, voltage, and mean current on MRR and SR for stainless steel. They concluded that Taguchi, ANOVA, and GRA methods are highly effective for identifying significant process parameters and optimizing machining performance. Ay and Etyemez [12] optimized WEDM parameters for DIN 1.2316 plastic mold steel using Taguchi and GRA, reporting that a 9 mm/min table feed rate, 8 µs pulse-on time, and 8 µs pulse-off time improved dimensional accuracy and shape tolerance. Jagdale et al. [13] applied Taguchi's L9 design and ANOVA for WEDM of Ti-6Al-4V alloy, identifying peak current as the most significant factor (72.75% contribution to MRR). Both peak current and pulse-on time were found to dominate surface roughness (Ra), with lower energy inputs favouring improved surface finish. Mohankumar et al. [14] combined RSM and GRA to optimize EDM parameters for Ti-6Al-4V alloy, achieving a maximum MRR of 8.52 $mm^3$/min at 22 A and a minimum SR of 2.65 µm at 12 A. ANOVA confirmed that peak current and Toff were the most significant factors, with confirmation experiments validating the model's reliability ($R^2$ = 98.9%). Seidi et al. [15] used the hybrid MEREC-WASPAS method to determine optimal WEDM parameters (wire feed speed of 2 cm/s, wire tension of 2.5 kg, and generator power of 10%). Roughness was the most critical factor (89% weight), and the optimal settings improved surface quality, hardness, and dimensional accuracy. Jithendra et al. [16] developed the ANFIS-SO model, which achieved 99% accuracy in predicting surface roughness, MRR, and residual stress of Monel 400 alloy during WEDM, with significantly lower errors compared to conventional ANFIS models. Kumar et al. [17] reported that ANFIS outperformed PSO in optimizing WEDM parameters for NiTi-SMA. The optimal ANFIS settings (*Ip* = 11.5 A, *Ton* = 125 µs, *Toff* = 58 µs, $S_V$ = 55 V, wire feed = 2 mm/min) improved surface morphology and minimized micro-cracks and potholes, as confirmed by FESEM and EDS analysis. Vora et al. [18] demonstrated that powder-mixed EDM with nano-graphene enhanced machining of Nitinol SMA by increasing MRR and reducing SR and

dimensional deviation. Taguchi's L9 design and ANOVA identified powder concentration, pulse-on time, and pulse-off time as key factors, while FESEM showed improved surface morphology with fewer defects at 2 g/L nano-graphene concentration. Chaudhari et al. [19] showed that near-dry WEDM significantly improved the surface quality of Nitinol SMA, achieving a 41.56% reduction in SR compared to wet-WEDM, despite a slight 8.94% reduction in MRR. TLBO optimization identified Ton = 35 µs, Toff = 27 µs, and current = 2 A as optimal settings, while SEM confirmed fewer surface defects and improved morphology. Wire-EDM of Ni55.8Ti alloy, optimized by Magabe et al. [20] using Taguchi's design and NSGA-II, achieved accurate prediction (±6% error) with improved MRR (0.021 g/min) and enhanced surface finish ($R_z$ = 6.2 µm) with reduced defects. Adedeji et al. [21] proposed a TP-GWO-DFA hybrid scheme effectively optimized wire-EDM of Nitinol-60, achieving a 398% gain in CR with minimal losses in $R_z$, $R_t$, SCD, and RLT, demonstrating efficient parameter selection with reduced data requirements. Wire-EDM of Inconel 625 optimized by Karsh and Singh [22] using Taguchi–grey relational analysis and validated by confirmation tests achieved improved cutting rate, surface finish, dimensional accuracy, and wire wear control. WEDM of Ni54.1Ti45.9 alloy with zinc-coated brass wire was effectively modelled by Gupta et al. [23] using ANN and optimized with a GA–ANN hybrid, achieving accurate prediction of MRR and surface roughness and significant improvement in surface quality under optimal parameters. WEDM of Nitinol rods combined with FESEM analysis and deep learning models showed that DenseNet achieved the highest accuracy (100%) in predicting surface morphology, demonstrating the effectiveness of the proposed approach for reliable prediction in manufacturing with limited data [24].

Despite extensive studies on WEDM of conventional metals, research on WEDM of NiTi shape memory alloys is still limited, particularly in the area of multi-objective optimization of material removal rate (MRR) and surface roughness (SR). Most prior works rely on single-objective or basic statistical methods, such as Taguchi and ANOVA, with minimal focus on integrating advanced hybrid techniques like Response Surface Methodology (RSM) with Grey Relational Analysis (GRA) for predictive modeling. Moreover, there is a noticeable lack of studies analyzing the combined influence of spark on-time ($S_{ON}$), spark off-time ($S_{OFF}$), servo voltage ($S_V$), and wire feed ($W_F$) on both productivity and surface quality. This highlights the need for robust empirical models and hybrid optimization frameworks tailored specifically for NiTi shape memory alloys to simultaneously achieve higher machining efficiency and superior surface integrity.

## 2. MATERIALS AND METHODS

The current experimental study was conducted using a Wire Electric Discharge Machine (Make: Electronica Machine Tool), which comprises four main systems: drive, positioning, dielectric, and power supply at NIT Kurukshetra. The power system includes pulse control, short-circuit protection, and high-voltage DC circuits. The dielectric system consists of a water chiller, filtration, a deionization unit, and a deionized water tank. The CNC-based positioning system operates adaptively, automatically adjusting when the wire nears the workpiece or when debris causes a short circuit. The drive system ensures continuous wire feed with proper tension, minimizing vibration, taper, and wire breakage. Wire guidance is provided by diamond or sapphire guides. Deionized water was used as the dielectric fluid, and a 0.25 mm diameter diffused brass wire served as the cutting tool. Ni51.59Ti Shape Memory Alloy was selected as the workpiece material for this study due to its unique shape memory and superelastic properties, making it highly valuable in aerospace, biomedical, automotive, and electronic applications. Its ability to recover shape after deformation and resist fatigue contributes to its widespread use in advanced engineering and medical devices. A full factorial design ($3^k$) was employed to plan the experimental runs, where *k* represents the number of controlled parameters. Four factors, such as spark-on time, spark-off time, wire feed, and servo voltage, were studied at three levels each, resulting in 29 experimental runs. Table 1(a) presents the parametric combinations for these tests, which were selected based on a detailed literature review. Table 1(b) represents the fixed criteria for the present study. Surface roughness (SR) was chosen as the performance metric, measured using a Surface Profilometer from Accretech Electronic Ltd., while material removal rate (MRR) was calculated by determining the volume of material removed per unit of time. This is determined by measuring the weight difference of the workpiece before and after machining, along with the machining time and material density.

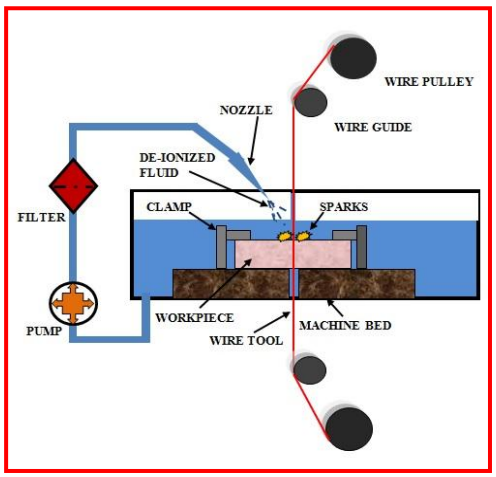


**Fig. 1.** Schematic diagram of WEDM

**Table 1 a).** Wire-EDM process parameters used in the present work

| Input process parameters | | | |
|---|---|---|---|
| **Parameters** | **Levels** | | |
| | **L1** | **L2** | **L3** |
| Spark-on time - $S_{ON}$ (µs) | 105 | 115 | 125 |
| Spark-off time - $S_{OFF}$ (µs) | 40 | 50 | 60 |
| Wire Feed - $W_F$ (m/min) | 7 | 9 | 11 |
| Servo voltage - $S_V$ (V) | 30 | 50 | 70 |

**Table 1 b).** Fixed process parameters

| Parameters | Value | Fixing criteria |
|---|---|---|
| Dielectric fluid | De-ionized Water | Literature review and pilot experiments |
| Peak Voltage | 200 V | |
| Water Pressure | 1 KPa | |
| Wire Tension | 7 N | |
| Servo Feed | 2050 mm/min | |

## 3. RESULTS AND DISCUSSION

The main experiments are carried out according to the BBD (Table 2) of RSM, to explore the effects of $S_{ON}$, $S_{OFF}$, $W_F$, and $S_V$ on process performance characteristics. The ranges and levels of input parameters and fixed parameters for the main experiments are illustrated in Table 1 a). The main experiments are performed with two replications. The mean values of response parameters are depicted in Table 2. It is found that the highest value of MRR (~8.312 $mm^3$/min) and SR (~3.4µm) are achieved for the parametric setting ($S_{ON}$=125µs, $S_{OFF}$ = 40 µs, $W_F$ = 9 m/min, $S_V$ = 50 V). Lowest value of MRR (~0.966 $mm^3$/min) achieved for parametric-setting ($S_{ON}$ = 105 µs, $S_{OFF}$ = 60 µs, $W_F$ = 9m/min, $S_V$ = 50 V). Parametric setting ($S_{ON}$ = 105 µs, $S_{OFF}$ = 50 µs, $W_F$= 9 m/min, $S_V$ = 30V) gives a minimum value of SR that is 0.721 µm. The experimental results are analyzed utilizing Design Expert software (version 7.0.0) for analysis of variance (ANOVA), parametric optimization, and mathematical model development.

**Table 2.** Experimental results for MRR & SR

| **Run** | **$S_{ON}$** (µs) | **$S_{OFF}$** (µs) | **$W_F$** (m/min) | **$S_V$** (V) | **MRR** ($mm^3$/min) | **S/N ratio for MRR** | **SR** (µm) | **S/N ratio for SR** |
|---|---|---|---|---|---|---|---|---|
| 1 | 105 | 40 | 9 | 50 | 2.85 | 9.0 | 1.6 | -4.0 |
| 2 | 125 | 40 | 9 | 50 | **8.31** | 18.3 | **3.4** | -10 |
| 3 | 105 | 60 | 9 | 50 | **0.96** | -0.30 | 0.8 | 1.72 |
| 4 | 125 | 60 | 9 | 50 | 6.00 | 15.5 | 3.1 | -10 |
| 5 | 115 | 50 | 7 | 30 | 5.84 | 15.3 | 2.4 | -7.7 |
| 6 | 115 | 50 | 11 | 30 | 3.84 | 11.7 | 1.5 | -3.5 |
| 7 | 115 | 50 | 7 | 70 | 3.43 | 10.7 | 3.0 | -9.7 |
| 8 | 115 | 50 | 11 | 70 | 3.41 | 10.6 | 2.8 | -8.9 |
| 9 | 105 | 50 | 9 | 30 | 2.52 | 8.0 | **0.7** | 2.8 |
| 10 | 125 | 50 | 9 | 30 | 6.26 | 15.9 | 2.4 | -7.9 |
| 11 | 105 | 50 | 9 | 70 | 2.32 | 7.3 | 1.4 | 4.7 |
| 12 | 125 | 50 | 9 | 70 | 5.87 | 15.3 | 3.0 | 81.7 |
| 13 | 115 | 40 | 7 | 50 | 5.01 | 14.0 | 2.8 | 64.2 |
| 14 | 115 | 60 | 7 | 50 | 3.03 | 9.6 | 2.4 | 35.7 |
| 15 | 115 | 40 | 11 | 50 | 5.42 | 14.6 | 2.8 | 68.2 |
| 16 | 115 | 60 | 11 | 50 | 3.00 | 9.5 | 2.1 | 21.2 |
| 17 | 105 | 50 | 7 | 50 | 2.56 | 8.1 | 1.6 | 6.9 |
| 18 | 125 | 50 | 7 | 50 | 7.91 | 17.9 | 3.2 | 108. |

**Table 2.** Experimental results for MRR & SR - *Table continued from the previous page*

| Run | $S_{ON}$ (µs) | $S_{OFF}$ (µs) | $W_F$ (m/min) | $S_V$ (V) | MRR ($mm^3$/min) | S/N ratio for MRR | SR (µm) | S/N ratio for SR |
|---|---|---|---|---|---|---|---|---|
| 19 | 105 | 50 | 11 | 50 | 2.72 | 8.7 | 0.9 | 0.65 |
| 20 | 125 | 50 | 11 | 50 | 6.40 | 16.1 | 3.0 | 86.7 |
| 21 | 115 | 40 | 9 | 30 | 4.14 | 12.4 | 2.3 | 29.1 |
| 22 | 115 | 60 | 9 | 30 | 4.02 | 12.1 | 1.7 | 10.1 |
| 23 | 115 | 40 | 9 | 70 | 5.76 | 15.0 | 2.5 | 40.6 |
| 24 | 115 | 60 | 9 | 70 | 1.95 | 5.8 | 2.7 | 54.4 |
| 25 | 115 | 50 | 9 | 50 | 5.13 | 14.2 | 2.7 | 60.1 |
| 26 | 115 | 50 | 9 | 50 | 5.76 | 15.2 | 2.6 | 48.4 |
| 27 | 115 | 50 | 9 | 50 | 5.78 | 15.2 | 2.9 | 74.7 |
| 28 | 115 | 50 | 9 | 50 | 5.96 | 15.5 | 2.9 | 80.5 |
| 29 | 115 | 50 | 9 | 50 | 5.88 | 15.3 | 2.6 | 49.9 |

### 3.1 ANOVA and Regression Model for MRR

As mentioned in the previous paragraph, the Design Expert software suggested a quadratic model for MRR. The ANOVA results for MRR are presented in Table 3. Based on the fit summary from the analysis, the developed model for MRR is found to be statistically significant. To eliminate non-significant terms, backward elimination with a 95% confidence interval was applied. A p-value less than 0.05 indicates that the model terms are significant. The overall model p-value is less than 0.0001, and the F-value is 24.59, confirming that the generated model is highly significant. According to the ANOVA results, the significant terms affecting MRR include the process variables $S_{ON}$, $S_{OFF}$, $S_V$, the interaction of $S_{OFF}$ and $S_V$, $S^2_{OFF}$, $W^2_F$, and $S^2_V$. The $R^2$ value of 0.9609 indicates that the model can explain 96.09% of the variation in the response. The Predicted $R^2$ (0.7942) shows good agreement with the Adjusted $R^2$ (0.9218). The Adequate Precision value (signal-to-noise ratio) of 17.810, which is much greater than the desirable minimum of 4, further validates the model. Among the variables, $S_{ON}$ shows the highest percentage contribution (63.79%), followed by $S_{OFF}$, $S_V$, and $W_F$. Fig. 2 shows the Box-Cox plot for MRR, which is used to determine the appropriate power transformation.

**Table 3.** ANOVA table for MRR

| Source | SS | DOF | MS | F-value | P-value |
|---|---|---|---|---|---|
| Model | 15.52 | 14 | 1.11 | 29.16 | <0.0001 |
| A- $S_{ON}$ | 10.49 | 1 | 10.49 | 276.04 | <0.0001 |
| B- $S_{OFF}$ | 0.50 | 1 | 0.50 | 13.11 | 0.0028 |
| C- $W_F$ | 0.46 | 1 | 0.46 | 12.05 | 0.0037 |
| D- $S_V$ | 1.55 | 1 | 1.55 | 40.80 | <0.0001 |
| $A^2$ | 1.64 | 1 | 1.64 | 43.18 | <0.0001 |
| $D^2$ | 0.74 | 1 | 0.74 | 19.34 | 0.0006 |
| Residual | 0.53 | 14 | 0.03 | | |
| Lack of Fit | 0.43 | 10 | 0.04 | 1.64 | 0.3348 |
| Pure Error | 0.10 | 4 | 0.02 | | |
| Cor Total | 16.05 | 28 | | | |

According to the foremost 'λ' value, a suggested transform is noted. This is found at the lowest point of the curve originating from the natural log of the residual sum of squares. At 95% C.I., the value of 'λ' is 1, then the software doesn't suggest a specific transformation. This plot depicts the value of 'λ' at the lowermost point, which gives the lowest residual sum of squares in the transformed model. The possibility of enhancements is greatest when the highest to lowest range of response value is larger than 3. The plot shows the minimum λ value as well as λ at 95% C.I. In order to find the value of λ, Fig. 2 shows a Box-Cox plot for MRR. This plot reveals that variation in λ with the natural log of the residual sum of squares (residuals) is polynomial in nature. Thus, the suggested value of λ = 1 in power transformation for MRR is used for ANOVA. Fig. 3 depicts a normal probability plot of residuals for MRR. This plot definitely depicts that the residuals are grouped about a straight line, which means the error of the model is normally distributed. Fig. 4 depicts the predicted vs actual plot for MRR. It is found that most of the points are closer to the line, which justifies the predictive capability of the models. Hence, it may be concluded that the anticipated values obtained by the models are consistent with experimental values.

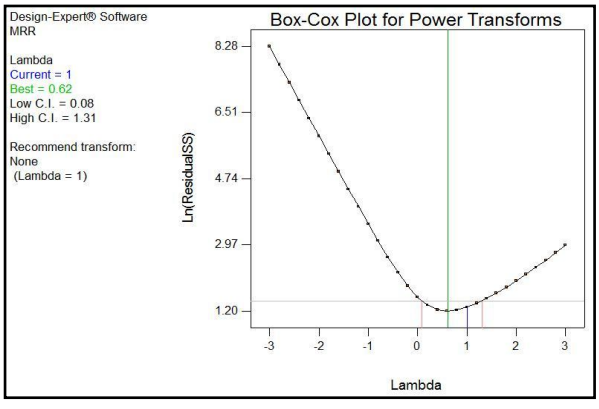


**Fig. 2.** Box-Cox plots for material removal rate

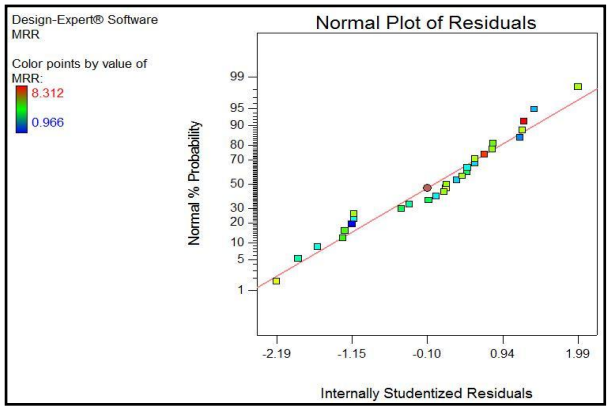


**Fig. 3:** Normal % probability plots for MRR

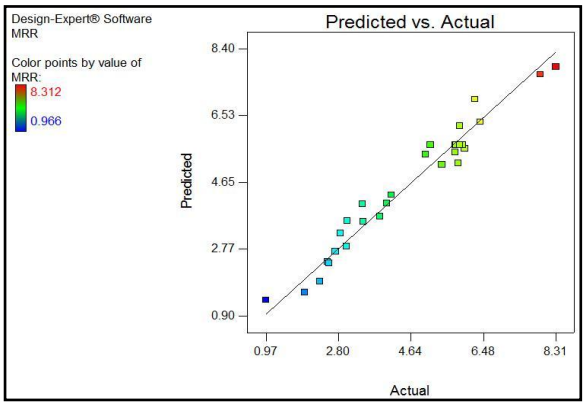


**Fig. 4.** Actual Vs predicted plots for MRR

The influence of the process variable on the MRR has been calculated using Design Expert 7.0 software, on the basis of the suggested second-order polynomial model. Eq. 1 depicts the mathematical correlation between MRR and coded factor, and MRR and actual process variables, respectively. This equation can be used for the prediction of MRR at a specified level of every factor. Regression equation in terms of coded factor for material removal rate:

$$MRR = 5.70 + 2.23 \times A - 1.04 \times B - 0.25 \times C - 0.32 \times D - 0.92 \times B \times D - 0.86 \times B^2 - 0.59 \times C^2 - 0.99 \times D^2 \quad (1)$$

### 3.2 ANOVA and Regression Model for Surface Roughness

As discussed in the previous section, the Design Expert software recommended a quadratic model for SR. The ANOVA results for SR are summarized in Table 4. Based on the fit summary, the developed model for SR is found to be statistically significant. To remove non-significant terms, backward elimination with a 95% confidence interval was applied. A p-value less than 0.05 indicates the significance of model terms. The overall model p-value is less than 0.0001, and the F-value of 29.16 confirms that the generated model is highly significant. According to the ANOVA outcomes, the significant process variables for SR are $T_{ON}$, $T_{OFF}$, $W_F$, $S_V$, $T^2_{ON}$, and $S^2_V$. The $R^2$ value of 0.9668 indicates that the model explains 96.68% of the variation in the response. The Predicted $R^2$ (0.8363) shows good agreement with the Adjusted $R^2$ (0.9337). The Adequate Precision value of 18.566, which is well above the desirable minimum of 4, further validates the model. Among the variables, $T_{ON}$ contributes the most (65.35%), followed by $T_{OFF}$, $S_V$, and $W_F$. Fig. 5 depicts the Box-Cox plot for SR. It is utilized to calculate the power transform [25].

**Table 4.** ANOVA table for SR

| Source | SS | DOF | MS | F-value | P-value |
|---|---|---|---|---|---|
| Model | 90.21 | 14 | 6.44 | 24.59 | <0.0001 |
| A- $S_{ON}$ | 59.89 | 1 | 59.89 | 228.5 | <0.0001 |
| B- $S_{OFF}$ | 13.09 | 1 | 13.09 | 49.95 | <0.0001 |
| C- $W_F$ | 0.74 | 1 | 0.74 | 2.84 | 0.1144 |
| D- $S_V$ | 1.26 | 1 | 1.26 | 4.81 | 0.0457 |
| BD | 3.41 | 1 | 3.41 | 13.01 | 0.0029 |
| $B^2$ | 4.78 | 1 | 4.78 | 18.22 | 0.0008 |
| $C^2$ | 2.28 | 1 | 2.28 | 8.70 | 0.0106 |
| $D^2$ | 6.40 | 1 | 6.40 | 24.43 | 0.0002 |
| Residual | 3.47 | 14 | 0.26 | | |
| Lack of Fit | 3.24 | 10 | 0.32 | 3.01 | 0.1501 |
| Pure Error | 0.43 | 4 | 0.11 | | |
| Cor Total | 93.88 | 28 | | | |

In order to find the value of λ Fig. 5 shows Box-Cox plot for SR. This plot reveals that variation in λ with the natural log of residual sum of squares (Ln(residuals)) is polynomial in nature. Thus, the suggested value of λ = 1 in power transformation for SR and it is used for ANOVA. Fig. 6 depicts a normal probability plot of residuals for SR. This plot definitely depicts that residuals are grouped about a straight line, which means the error of the model is normally distributed. Fig. 7 depicts the predicted vs actual plot for SR. The influence of the process parameters on the SR has been calculated using 'Design Expert 7.0 software', based on the proposed second-order polynomial model. Eq. 2 depicts the mathematical correlation between SR and coded factor, and SR and actual process variables, respectively. This equation can be used for the prediction of SR at a specified level of every factor. Regression equation in terms of coded factor for surface roughness:

$$SR = 2.80 + 0.94 \times A - 0.20 \times B - 0.20 \times C + 0.36 \times D - 0.50 \times A^2 - 0.34 \times D^2 \quad (2)$$

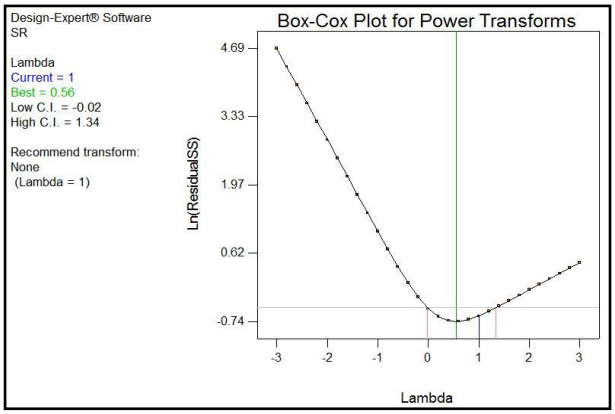


**Fig. 5.** Box-Cox plots for SR

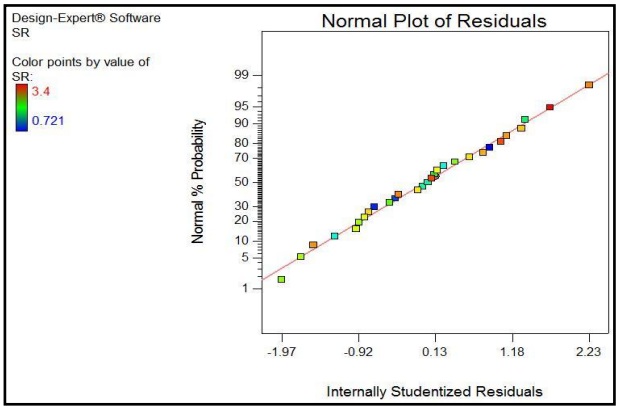


**Fig. 6.** Normal probability plots for SR

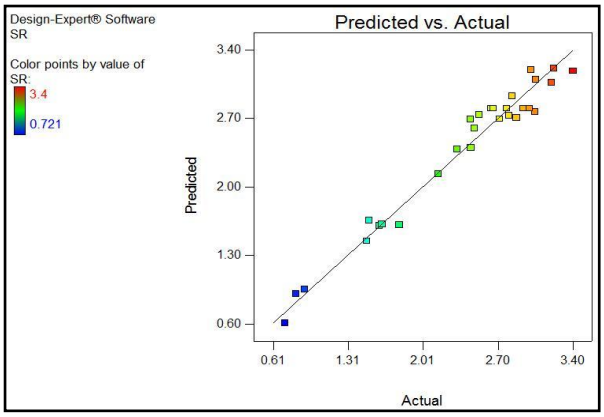


**Fig. 7.** Actual Vs predicted plots for SR

### 3.3 Grey Relational Analysis

This section represents an application of Grey Relational Analysis (GRA) to obtain multi-response optimization of WEDM process parameters for Ni-Ti SMA machining. The graphical illustration of various steps used in GRA is shown in Fig. 8.

Multi-response optimization theory using GRA is used for optimizing the parameters when only partial information is known. GRA is a simple, liable and efficient method of assessing the optimum process parameters for machining of Ni-Ti SMA and multi-response optimization of process performance characteristics. The GRA model expresses the relationship between two elements in a system, and the grey relational grade (GRG) is greater if the relationship between two system aspects is larger.

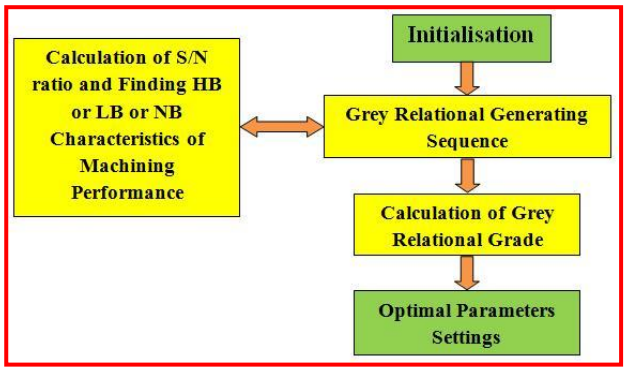


**Fig. 8.** Flow chart for Grey Relational Analysis

A step-by-step procedure to calculate GRG is described as follows:

*Stage 1: Determination of S/N ratio:* The initial step in Grey Relation Analysis is the determination of the S/N-ratio of correlated outputs by subsequent rule [26]:

I. Larger the Better (LB):

$$S/N\ ratio\ (\lambda) = -10\log_{10}\frac{1}{p}\sum_{k=1}^{p} 1/y_{kl}^2 \qquad (3)$$

where are: p - total no. of iterations and $y_{kl}^2$ - experimental outputs data with k=1, 2, 3….p, and l=1, 2, 3….m. MRR needs to be maximized for machining during WEDM of SMA. Owing to this, LB formula is applied for MRR.

II. Smaller the Better (SB):

$$S/N\ ratio\ (\lambda) = -10\log_{10}\frac{1}{p}\sum_{k=1}^{p} y_{kl}^2 \qquad (4)$$

where are: p - total no. of iterations and $y_{kl}^2$ - experimental response data with k=1, 2, 3….p, and l=1, 2, 3….m. SR needs to be minimized for machining during WEDM of SMA. Owing to this, LB formula is applied for MRR.

*Stage 2: Normalization of S/N ratio:* After determining the S/N ratio implied for associated outputs, the next step in GRA is normalization of the estimated S/N ratio. Normalization of the dataset is essential owing to the fact that units and ranges in individual data sets may differ from the remaining. Therefore, linear normalization of the dataset is completed by transporting the primary order into a similar order. In GRA, this reprocessing of the S/N ratio is termed as grey relational generation [27]. $y_{kl}$ is transformed into a comparability sequence $x_{kl}$ by the subsequent equations:

I. LB approach (MRR):

$$x_{kl} = \frac{y_{kl} - \min(y_{kl})}{\max(y_{kl}) - \min(y_{kl})} \quad (5)$$

II. SB approach (SR):

$$x_{kl} = \frac{\max(y_{kl}) - y_{kl}}{\max(y_{kl}) - \min(y_{kl})} \quad (6)$$

*Stage 3: Determination of Grey Relational Coefficient (GRC):* GRC is then estimated for the normalized dataset to establish the connection between the utmost (elite=1) and real experimental results. The grey relational coefficient is defined by Eq. 7:

$$\eta[x_0(q), x_i(q)] = \frac{\Delta \min + \in \Delta max}{\Delta_{0i}(q) + \in \Delta max} \quad (7)$$

where are: *i*=1, 2, 3…….p and *q*=1, 2, 3……m, *i* is the number of experiments, *q* indicates the overall outputs. $x_0(q)$ indicate reference sequence; $x_i(q)$ relates the overall responses. $\Delta_{oi}(q)$ is the absolute value of the difference between $x_0(q)$ and $x_i(q)$. $\Delta min$ and $\Delta max$ are the lowest and highest values of $x_i(q)$, and it is also termed as the quality loss function. 'ε' is the unique coefficient, and its value ranges between '0' to '1' with systematic actual need.

*Stage 4: Determination of Grey relational Grade (GRG):* The 4th stage in GRA is the determination of 'GRG'. It is the mean sum of GRC, which is calculated by Eq. 8:

$$\lambda(x_0, x_i) = \frac{1}{e}\sum_1^e \eta[x_0(q), x_i(q)] \quad (8)$$

where are: $\eta(x_0, x_j)$ denotes the GRG of $j^{th}$ trial, even though 'e' denotes total no. of outcomes. Further 'weights' are allocated to the specific 'GRGs' owing to the effective responses on the entire process performance. The substantial 'GRG' is termed as weighted 'GRG' and calculated by Eq. 9:

$$\lambda_w(x_0, x_i) = \frac{1}{e}\sum_1^e w_1\left(\eta\left(x_0(q), x_i(q)\right)\right) + w_2\left(\eta\left(x_0(q), x_i(q)\right)\right) \quad (9)$$

where are: $w_1$ and $w_2$ are the weights allocated to the specific responses.

*Stage 5: Computation of optimum parameters and their levels:* Previously, the weighted 'GRG' for each number is obtained; these GRG are chosen as outcomes for further investigation. The larger-the-better method was used for inspecting the 'GRG'. The larger 'GRG' represents greater functioning; so the optimum parameters and their level can be considered basing itself of 'GRG' value. The average 'GRA' at every level is estimated for singly processed variables and the level with the highest 'GRG' is chosen as the optimum. Table 5 represents the Grey relational coefficient and grey relational grade for MRR and SR. Table 6 shows the validation of GRA results.

**Table 5.** Grey relational coefficient and grey relational grade for MRR and SR

| Run | GRC for MRR | GRC for SR | GRG | Rank | S/N ratio for GRG |
|---|---|---|---|---|---|
| 1 | 0.499 | 0.507 | 0.502 | 25 | -5.97103 |
| 2 | 0.333 | 1 | 0.666 | 4 | -3.52183 |
| 3 | 1 | 0.352 | 0.676 | 2 | -3.39562 |
| 4 | 0.371 | 0.926 | 0.648 | 5 | -3.76051 |
| 5 | 0.374 | 0.702 | 0.538 | 22 | -5.374 |
| 6 | 0.438 | 0.486 | 0.462 | 27 | -6.7036 |
| 7 | 0.459 | 0.876 | 0.667 | 3 | -3.50937 |
| 8 | 0.460 | 0.800 | 0.630 | 7 | -4.00786 |
| 9 | 0.528 | 0.333 | 0.430 | 29 | -7.31231 |
| 10 | 0.365 | 0.711 | 0.538 | 21 | -5.37451 |
| 11 | 0.551 | 0.482 | 0.516 | 24 | -5.73987 |
| 12 | 0.373 | 0.863 | 0.618 | 9 | -4.17513 |
| 13 | 0.395 | 0.808 | 0.602 | 13 | -4.40759 |
| 14 | 0.485 | 0.701 | 0.593 | 15 | -4.53507 |
| 15 | 0.384 | 0.821 | 0.602 | 12 | -4.39393 |
| 16 | 0.487 | 0.627 | 0.557 | 18 | -5.07793 |
| 17 | 0.525 | 0.511 | 0.518 | 23 | -5.7101 |
| 18 | 0.339 | 0.935 | 0.637 | 6 | -3.91488 |
| 19 | 0.509 | 0.368 | 0.438 | 28 | -7.15111 |
| 20 | 0.363 | 0.877 | 0.620 | 8 | -4.14891 |
| 21 | 0.425 | 0.670 | 0.547 | 20 | -5.22792 |
| 22 | 0.430 | 0.545 | 0.487 | 26 | -6.23417 |
| 23 | 0.376 | 0.722 | 0.549 | 19 | -5.20278 |
| 24 | 0.605 | 0.775 | 0.690 | 1 | -3.22029 |
| 25 | 0.392 | 0.795 | 0.593 | 14 | -4.53044 |
| 26 | 0.376 | 0.753 | 0.564 | 17 | -4.96361 |
| 27 | 0.376 | 0.842 | 0.608 | 11 | -4.30968 |
| 28 | 0.372 | 0.859 | 0.615 | 10 | -4.21293 |
| 29 | 0.373 | 0.759 | 0.566 | 16 | -4.93883 |

**Table 6.** Validation results for GRA

| Response Parameters | Modified Process Inputs | | | | Predicted values | Experimental values | % error |
|---|---|---|---|---|---|---|---|
| | $T_{ON}$ | $T_{OFF}$ | $W_F$ | $S_V$ | | | |
| ***Trail 1:*** | | | | | | | |
| MRR | 125 | 56 | 8 | 30 | 6.982 | 7.138 | 2.185 |
| SR | | | | | 2.528 | 2.659 | 4.926 |
| ***Trail 2:*** | | | | | | | |
| MRR | 125 | 56 | 8 | 30 | 6.982 | 7.105 | 1.731 |
| SR | | | | | 2.528 | 2.554 | 1.018 |

$$MRR = 5.70 + 2.23 \times A - 1.04 \times B - 0.25 \times C - 0.32 \times D - 0.11 \times A \times B - 0.42 \times A \times C - 0.047 \times A \times D - 0.11 \times B \times C - 0.92 \times B \times D + 0.49 \times C \times D - 0.33 \times A^2 - 0.86 \times B^2 - 0.59 \times C^2 - 0.99 \times D^2 \quad (10)$$

$$MRR = -133.7 + 1.23 \times Son + 1.15 \times Soff + 4.60 \times Wf + 0.37 \times Sv - 1.07 \times 10^{-3} \times Son \times Soff - 0.02 \times Son \times Wf - 2.32 \times 10^{-4} \times Son \times Sv - 5.48 \times 10^{-3} \times Soff \times Wf - 4.61 \times 10^{-3} \times Soff \times Sv + 0.01 \times Wf \times Sv - 3.29 \times 10^{-3} \times Son^2 - 8.58 \times 10^{-3} \times Soff^2 - 0.14 \times Wf^2 - 2.48 \times 10^{-3} \times Sv^2 \quad (11)$$

$$SR = 2.80 + 0.94 \times A - 0.20 \times B - 0.20 \times C + 0.36 \times D + 0.14 \times A \times B + 0.14 \times A \times C - 0.05 \times A \times D - 0.08 \times B \times C + 0.18 \times B \times D + 0.18 \times C \times D - 0.50 \times A^2 - 0.11 \times B^2 - 0.07 \times C^2 - 0.34 \times D^2 \quad (12)$$

$$SR = -63.84 + 1.13 \times Son - 0.08 \times Soff - 0.54 \times Wf + 0.05 \times Sv + 1.44 \times 10^{-3} \times Son \times Soff + 6.87 \times 10^{-3} \times Son \times Wf - 2.92 \times 10^{-4} \times Son \times Sv - 4.27 \times 10^{-3} \times Soff \times Wf + 9.12 \times 10^{-4} \times Soff \times Sv + 4.41 \times 10^{-3} \times Wf \times Sv - 5.03 \times 10^{-3} \times Son^2 - 1.08 \times 10^{-3} \times Soff^2 - 0.02 \times Wf^2 - 8.41 \times 10^{-4} \times Sv^2 \quad (13)$$

### 3.4 Contour Plots of GRG

Contour plots of GRG are shown in Fig. 9 a) to Fig. 9 b). In GRA, the rank is decided by the GRG value. Greater the GRG, better will be the rank of that particular setting. From Fig. 9 (a), it is depicted that for spark on time is longer and spark off time is shorter, the combination gives a higher value of GRG. From Fig. 9 (b), it is depicted that for lowest value of GRG can be obtained from the combination of a longer pulse off time and a lower servo voltage value.

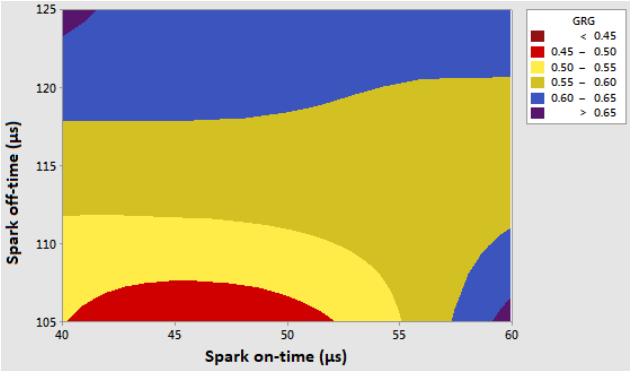


a)

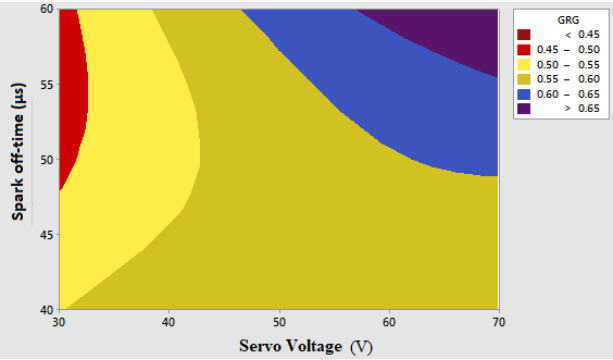


b)

**Fig. 9.** Contour plots of GRG

## 4. CONCLUSION

The present study focused on the machining of Ni51.59Ti shape memory alloy using WEDM by analyzing the influence of key process parameters, spark on-time ($S_{ON}$), spark off-time ($S_{OFF}$), wire feed ($W_F$), and servo voltage ($S_V$) on MRR and SR. Response Surface Methodology combined with Box-Behnken Design was effectively employed to develop empirical models and perform ANOVA analysis, which confirmed the statistical significance of $S_{ON}$ as the most dominant factor for both MRR and SR, followed by $S_{OFF}$, $S_V$, and $W_F$. The developed quadratic models demonstrated high predictive accuracy with $R^2$ values of 0.9609 and 0.9668 for MRR and SR, respectively. Multi-objective optimization using Grey Relational Analysis successfully determined the optimal parameter setting at $S_{ON}$ = 115 µs, $S_{OFF}$ = 60 µs, $W_F$ = 9 mm/min, and $S_V$ = 70 V, achieving a desirable balance between maximizing MRR and minimizing SR. Validation experiments confirmed the reliability of the optimized parameters with minimal error margins. The study highlights that a longer spark-on time coupled with a shorter spark-off time significantly enhances machining efficiency, whereas servo voltage and wire feed exert secondary yet notable effects on surface quality. This research can be extended by incorporating advanced hybrid optimization techniques, such as genetic algorithms or machine learning-based predictive models, to further refine the parameter selection process.

## CONFLICTS OF INTEREST

The authors declare no conflict of interest.

## REFERENCES

[1] P.K. Karsh, H. Singh, Optimization of process parameters for surface roughness of Inconel

625 in wire EDM by using Taguchi method. *IOSR Journal of Mechanical and Civil Engineering*, 3 (3) (2016) 58-63. https://doi.org/10.9790/1684-15010030358-63

[2] C. O'Hara, M. McAfee, R. Raghavendra, D. Tormey, An additive manufacturing assisted electric discharge machining technique to produce complex, thin-walled, injection mould cavities in 316 L stainless steel. *Additive Manufacturing*, 105, 2025: 104800. https://doi.org/10.1016/j.addma.2025.104800

[3] K. Raju, M. Balakrishnan, C.B. Priya, M. Sivachitra, D. Narasimha Rao, Parametric optimization of wire electrical discharge machining in AA7075 metal matrix composite. *Advances in Materials Science and Engineering*, 2022, 2022: 4438419. https://doi.org/10.1155/2022/4438419

[4] F. Gillani, T. Zahid, S. Bibi, R.S.U. Khan, M.R. Bhutta, U. Ghafoor, Parametric optimization for quality of electric discharge machined profile by using multi-shape electrode. *Materials*, 15(6), 2022: 2205. https://doi.org/10.3390/ma15062205

[5] K.H. Ho, S.T. Newman, S. Rahimifard, R.D. Allen, State of the art in wire electrical discharge machining (WEDM). *Inter. Journal of Machine Tools and Manufacture*, 44(12-13), 2004: 1247-1259. https://doi.org/10.1016/j.ijmachtools.2004.04.017

[6] D.A.N. Scott, S. Boyina, K.P. Rajurkar, Analysis and optimization of parameter combinations in wire electrical discharge machining. *International Journal of Production Research*, 29(11), 1991: 2189-2207. https://doi.org/10.1080/00207549108948078

[7] H.O. González-Rojas, J.C. Miranda-Valenzuela, J. de Dios Calderón-Najera, Optimization of Cutting Parameters for Energy Efficiency in Wire Electrical Discharge Machining of AISI D2 Steel. *Applied Sciences*, 14(11), 2024: 4701. https://doi.org/10.3390/app14114701

[8] A.K. Srivastava, P. Pal, A. Pal, B.K. Singh, R. Kumar, A. Kumar, Parametric evaluation & optimization of wire-EDM process for machining of super alloy materials (EN-24 steel) in terms of surface integrity and material removal rate. *AIP Conference Proceedings,* 3221(1), 2024: 020033. https://doi.org/10.1063/5.0235844

[9] S.A. El-Bahloul, Optimization of wire electrical discharge machining using statistical methods coupled with artificial intelligence techniques and soft computing. *SN Applied Sciences*, 2, 2020: 49. https://doi.org/10.1007/s42452-019-1849-6

[10] S. Seshaiah, D. Sampathkumar, M. Mariappan, A. Mohankumar, G. Balachandran, M. Kaliyamoorthy, B. Rajendran, R. Gopal, Optimization on material removal rate and surface roughness of stainless steel 304 wire cut EDM by response surface methodology. *Advances in Materials Science and Engineering*, 2022, 2022: 6022550. https://doi.org/10.1155/2022/6022550

[11] K. Natarajan, H. Ramakrishnan, A. Gacem, V. Vijayan, K. Karthiga, H.E. Ali, B. Prakash, A. Mekonnen, Study on optimization of WEDM process parameters on stainless steel. *Journal of Nanomaterials,* 2022, 2022: 6765721. https://doi.org/10.1155/2022/6765721

[12] M. Ay, A. Etyemez, Optimization of the effects of wire EDM parameters on tolerances. *Emerging Materials Research*, 9(2), 2020: 527-531. https://doi.org/10.1680/jemmr.20.00076

[13] M. Jagdale, N. Ambhore, R. Chaudhari, A. Kulkarni, M. Abdullah, Experimental investigation of process parameters in Wire-EDM of Ti-6Al-4 V. *Scientific Reports*, 15, 2025: 5652. https://doi.org/10.1038/s41598-025-90486-2

[14] V. Mohankumar, M.S.S. Kumar, A. Karthik, A.K. Bojer, E. Ali, S.S. Ghoneim, A.B. Abou Sharaf, Optimizing EDM process parameters with the use of GRA-based RSM for machining titanium alloy. *Results in Engineering*, 26, 2025: 104903. https://doi.org/10.1016/j.rineng.2025.104903

[15] M. Seidi, S. Yaghoubi, F. Rabiei, Multi-objective optimization of wire electrical discharge machining process using multi-attribute decision making techniques and regression analysis. *Scientific Reports*, 14, 2024: 10234. https://doi.org/10.1038/s41598-024-60825-w

[16] T. Jithendra, S. Sharief Basha, R. Das, R. Gajjela, Modeling and optimization of WEDM of monel 400 alloy using ANFIS and snake optimizer: A comparative study. *Proceedings of the Institution of Mechanical Engineers, Part C: Journal of Mechanical Engineering Science*, 238(5), 2024: 1573-1589.

https://doi.org/10.1177/0954406223118720
7

[17] L. Kumar, A. Goyal, V.K. Pathak, Prediction and optimization of WEDM parameters for machining of NiTi-shape memory alloy using ANFIS-PSO approach. *Discover Applied Sciences*, 7, 2025: 249. https://doi.org/10.1007/s42452-025-06663-5

[18] J. Vora, S. Khanna, R. Chaudhari, V.K. Patel, S. Paneliya, D.Y. Pimenov, K. Giasin, C. Prakash, Machining parameter optimization and experimental investigations of nano-graphene mixed electrical discharge machining of nitinol shape memory alloy. *Journal of Materials Research and Technology,* 19, 2022: 653-668. https://doi.org/10.1016/j.jmrt.2022.05.076

[19] R. Chaudhari, A. Kevalramani, J. Vora, S. Khanna, V.K. Patel, D.Y. Pimenov, K. Giasin, Parametric optimization and influence of near-dry WEDM variables on nitinol shape memory alloy. *Micromachines*, 13(7), 2022: 1026. https://doi.org/10.3390/mi13071026

[20] R. Magabe, N. Sharma, K. Gupta, J.P. Davim, Modeling and optimization of Wire-EDM parameters for machining of Ni55.8Ti shape memory alloy using hybrid approach of Taguchi and NSGA-II. *The International Journal of Advanced Manufacturing Technology*, 102, 2019: 1703-1717. https://doi.org/10.1007/s00170-019-03287-z

[21] W.O. Adedeji, E. Fasina, M.K. Adeniran, K.A. Adedeji, J. Rajan, S.A. Oke, E.O. Oyetunji, Optimization of the wire electric discharge machining process of nitinol-60 shape memory alloy using Taguchi-Pareto design of experiments, grey-wolf analysis, and desirability function analysis. *Indonesian Journal of Industrial Engineering & Management*, 4(1), 2023: 28-50. http://dx.doi.org/10.22441/ijiem.v4i1.18087

[22] P.K. Karsh, H. Singh, Multi-characteristic optimization in wire electrical discharge machining of Inconel-625 by using Taguchi-grey relational analysis (GRA) approach: Optimization of an existing component/product for better quality at a lower cost. *Design and Optimization of Mechanical Engineering Products,* 2018: 281-303. https://doi.org/10.4018/978-1-5225-3401-3.ch014

[23] D.K. Gupta, A.K. Dubey, Modeling and optimization of Wire–EDM parameters for machining of $Ni_{54.1}Ti4_{5.9}$ shape memory alloy using hybrid approach. *Proceedings of the Institution of Mechanical Engineers, Part E: Journal of Process Mechanical Engineering*, 236(5), 2022: 2176-2186. https://doi.org/10.1177/0954408922108514

[24] V. Vakharia, J. Vora, S. Khanna, R. Chaudhari, M. Shah, D.Y. Pimenov, K. Giasin, P. Prajapati, S. Wojciechowski, Experimental investigations and prediction of WEDMed surface of Nitinol SMA using SinGAN and DenseNet deep learning model. *Journal of Materials Research and Technology*, 18, 2022: 325-337. https://doi.org/10.1016/j.jmrt.2022.02.093

[25] G.E.P. Box, N.R. Draper, Empirical model-building and response surfaces. *John Wiley & Sons*, 1987.

[26] A.N. Haq, P. Marimuthu, R. Jeyapaul, Multi response optimization of machining parameters of drilling Al/SiC metal matrix composite using grey relational analysis in the Taguchi method. *The International Journal of Advanced Manufacturing Technology*, 37(3), 2008: 250-255. https://doi.org/10.1007/s00170-007-0981-4

[27] R.S. Pawade, S.S. Joshi, Multi-objective optimization of surface roughness and cutting forces in high-speed turning of Inconel 718 using Taguchi grey relational analysis (TGRA). *The International Journal of Advanced Manufacturing Technology*, 56(1), 2011: 47-62. https://doi.org/10.1007/s00170-011-3183-z